International Journal of Research in Advent Technology, Vol.7, No.4, April 2019
E-ISSN: 2321-9637
Available online at www.ijrat.org

MHD Falkner-Skan Flow of a Radiative Casson Fluid past a Static/Moving Wedge with Viscous Dissipation

L. Wahidunnisa[1], K.Subbarayudu[2], S.Suneetha[3]*
Research Scholar[1], Research Scholar[2], Assistant Professor[3],
Department of Applied Mathematics, Yogi Vemana, University, Kadapa - 516005, A. P., INDIA[1, 2, 3]
Email: wahidayvu123@gmail.com, subbuyvu123@gmail.com, suneethayvu@gmail.com
** Corresponding Author*

Abstract- The main objective of the present attempt is to investigate the numerical solutions for the Falkner-Skan flow of two-dimensional radiative Magneto hydrodynamic Casson fluid past a static/moving wedge with convective boundary condition in the presence of porous medium. In addition to the effects of viscous dissipation and heat generation /absorption are also considered. A set of suitable local similarity transformations are used to non dimensionalize the governing equations of the present problem. The system of ordinary differential equations are tackled numerically by MATLAB bvp4c solver. The impact of involved parameters on velocity, temperature and concentration skin friction coefficient and the Nusselt number has been studied and numerical results are presented graphically and in tabular form. The numerical results are in good agreement with those of the results previously published in the literature.

Keywords: Casson fluid model, Convective Boundary condition, MHD, radiation, viscous dissipation.

NOMENCLATURE		Q	heat generation/absorption coefficient
u, v	velocity components in x and y directions respectively	q_r	radiative heat flux
T_w	The temperature at the boundary layer	k^*	absorption coefficient
C_w	The concentration at the boundary layer	f	similarity function
T_∞	The temperature at free stream	R	Radiation parameter
C_∞	The concentration at free stream	Pr	Prandtl number
B	magnetic field	Gr_x	Grashof number
p_y	yield stress of the fluid	Bi	Biot number
μ_b	plastic dynamic viscosity of the non-Newtonian fluid	Ec	Eckert number
π	product of the component of deformation	Cf_x	skin friction coefficient
B_0	Strength of the magnetic field	Nu_x	local Nusselt number
M	Magnetic parameter	**Greek symbols**	
K	Porosity parameter	β	Casson parameter
λ_T	thermal buoyancy parameter	σ	electrically conductivity
k_1	permeability of porous medium	ρ	fluid density
g	gravitational force due to	γ	moving wedge parameter
β_T	volumetric coefficient of thermal	Ω	total angle of the wedge
T	fluid temperature	ν	kinematic viscosity
k	thermal conductivity of the fluid	τ_w	wall skin friction
C_p	specific heat at constant pressure	q_w	wall heat flux

1. INTRODUCTION

The flow across a wedge shaped bodies have many engineering applications and also in the growth of fluid dynamics. The Falkner-Skan equation was first introduced by Falkner and Skan for boundary layer flow determined by a stream wise pressure gradient. The nonlinear third-order ordinary differential equation $f''' + ff' + \lambda\left(1 - f'^2\right) = 0$ with boundary conditions $f(0) = \beta,\ \ f'(0) = \gamma,\ \ f'(\infty) = 1$, where β is the strength of the mass transfer at the wall, $\lambda = \frac{2m}{m+1}$ is a stream wise pressure gradient which represent a two-dimensional incompressible laminar boundary layer flow. The original Falkner-Skan equation has $\beta = 0, \gamma = 0$ for an impermeable wedge flow. A lot of literature regarding the Falkner-Skan wedge flow can be found in the books by Schlichting and Gersten (2000) and Leal (2007). The wedge is triangular shaped and is used for separating two objects, one object hold in a plane and other lifting up. It converts the lateral force into a transverse splitting force. In addition, MHD plays an important role to control the heat transfer in boundary layer flow and metallurgical processes. Many investigators (Prasad, K. V.et al., (2013), Anuar Ishak, et al., (2009), Mourad F.Dimian, (2004), Nabil T. El-Dabe et al., (2015)),explored MHD effects on heat and mass transfer over a wedge for various conditions in different types of fluids. Abdulhameed et al., (2015) reported that the magnetic field decelerate the fluid flow while thermal radiation tends to enhance fluid temperature.

Convective Condition over a wedge with MHD was observed by Raju and Sandeep (2016).James et al., (2015) fed light on the effect of variable viscosity of nanofluid flow over a permeable wedge with chemical reaction and thermal radiation. Suneetha et al., (2008) studied thermal radiation effects on mhd free convection flow past an impulsively started vertical plate with variable surface temperature and concentration.

Suneetha and Bhaskar Reddy (2010) fed light on the radiation and mass transfer effects on mhd free Convection flow past a moving vertical cylinder embedded in porous medium. Ahmad and Khan (2013) examined the influence of viscous dissipation and heat generation or absorption on force convection flow of viscous fluid over a moving wedge subject to suction/injection. Imran Ullah et al., (2016) observed that the heat transfer rate decreases with an increase in Prandtl number in the presence of viscous dissipation in a moving wedge with heat transfer.

Motivated by such facts, the aim of the present article is to develop a mathematical model for steady two-dimensional Flakner-Skan wedge flow of MHD Casson fluid past a static/moving wedge in the presence of convective boundary condition and viscous dissipation. Also, radiation and heat generation are considered. With the help of similarity transformations, we transformed the derived governed equations as ordinary nonlinear differential equations. The results are determined by applying MATLAB bvp4c solver. Graphs are revealed and described for various non-dimensional governing parameters. By choosing the same parameters, we discussed about the skin friction coefficient and local Nusselt number with the assistance of tables separately.

2. MATHEMATICAL ANALYSIS

A steady Falkner-Skan flow of Casson fluid over a moving wedge through porous medium in the presence of MHD and viscous dissipation is considered. Here wedge is moving with the velocity $u_w(x) = U_w x^m$ and the free stream velocity $u_e(x) = U_\infty x^m$; where U_w and U_∞ are constants. $\lambda = \frac{2m}{m+1}$ is the Hartree pressure gradient parameter related to $\lambda = \frac{\Omega}{\pi}$ for the total angle Ω of the wedge (see Fig.1)

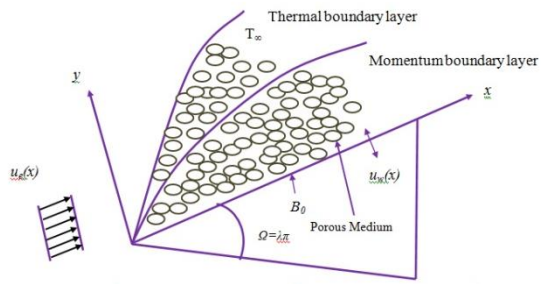

Figure1.physical model and coordinate system

The temperature and concentration at the boundary layer and free stream are represented by T_w; T_∞ and C_w; C_∞, respectively. A variable magnetic field $B(x) = B_0 x^{m-1/2}$ is applied in the direction of the flow as in Fig.1. It is also assumed that the induced magnetic field caused by the motion of electrically conducting fluid is neglected, as it is very small compared to magnetic field. Further, the buoyancy force generates due to temperature differences inside moving fluid, and is taken in momentum equation. The effect of heat generation/absorption with

convective boundary condition is also included in this study. Further, the wall of wedge is heated by variable temperature $T_w(x)=T_\infty + Ax^{2m}$ and free stream temperature is denoted by T_∞ .

The rheological equation of an isotropic and incompressible flow of a Casson fluid can be written as

$$\tau_{ij} = \left(\mu_b + \frac{P_y}{\sqrt{2\pi}}\right)2e_{ij} \quad when\, \pi > \pi_c ,$$

$$\tau_{ij} = \left(\mu_b + \frac{P_y}{\sqrt{2\pi}}\right)2e_{ij} \quad when\, \pi < \pi_c ,$$

P_y is known as yield stress of the fluid, mathematically expressed as $P_y = \frac{\mu_b\sqrt{2\pi}}{\beta}$. μ_b is known as plastic dynamic viscosity of the non-Newtonian fluid, π is the product of the component of deformation rate with itself (i.e. $\pi = e_{ij}\, e_{ij}$), where e_{ij} is the (i, j) th component of the deformation rate and π_c is the critical value based on the non-Newtonian model.

The rheological governing equations for momentum and energy are given as

$$\frac{\partial u}{\partial x} + \frac{\partial v}{\partial y} = 0 \tag{1}$$

$$u\frac{\partial u}{\partial x} + v\frac{\partial u}{\partial y} = u_e\frac{\partial u_e}{\partial x} + \nu\left(1+\frac{1}{\beta}\right)\frac{\partial^2 u}{\partial y^2} + \left(\frac{\sigma B^2(x)}{\rho} + \frac{\nu\phi}{k_1}\right)(u_e - u) \pm g\beta_T(T-T_\infty)\sin\frac{\Omega}{2} \tag{2}$$

$$u\frac{\partial T}{\partial x} + v\frac{\partial T}{\partial y} = \frac{\kappa}{\rho C_p}\frac{\partial^2 T}{\partial y^2} + \frac{1}{(\rho C_p)}\left(1+\frac{1}{\beta}\right)\left(\frac{\partial u}{\partial y}\right)^2 - \frac{1}{(\rho C_p)}\frac{\partial q_r}{\partial y} + \frac{Q(x)(T-T_\infty)}{\rho C_p} \tag{3}$$

Subject to the boundary conditions:

$$u = u_w(x),\ v = 0,\ -k\frac{\partial T}{\partial y} = h_f(T_w - T),\quad T_w(x) = T_\infty + Ax^{2m}\ \ at\ y = 0 \tag{4}$$

$$u \to u_e(x),\ T \to T_\infty \qquad as\ y \to \infty \tag{5}$$

where u and v denote the velocity components in x and y-directions respectively, ν is kinematic viscosity, β is the Casson parameter, σ is the electrically conductivity, B_0 is the strength of the magnetic field, ρ is the fluid density, ϕ is the porosity, k_1 is the permeability of porous medium, g is the gravitational force due to acceleration, '+' sign corresponds to assisting flow, '-' is for opposing flow, β_T is the volumetric coefficient of thermal expansion, T is the fluid temperature, k is the thermal conductivity of the fluid, C_p is the specific heat at constant pressure and $Q(x) = Q_0 x^{m-1}$ is heat generation/absorption coefficient. When material has a great extinction coefficient, it can be treated as optically thick. q_r is the radiative heat flux and is defined using the Rosseland approximation as

$$q_r = \frac{-4\sigma}{3k^*}\frac{\partial T^4}{\partial y}, \tag{6}$$

Where σ* is the Stefan–Boltzmann constant and k* is known as the absorption coefficient. We assumed that the temperature differences within the flow are sufficiently small such that T^4 may be expressed as a linear function of the free stream temperature T_∞. This is obtained by expanding T^4 in a Taylor series about T_∞ and neglecting higher order terms, we obtained

$$T^4 \approx T_\infty^4 + 4T_\infty^3 T - 4T_\infty^3 T_\infty, \tag{7}$$

$$\frac{\partial q_r}{\partial y} = \frac{\partial}{\partial y}\left(\frac{-4\sigma^*}{3k^*}\frac{\partial T^4}{\partial y}\right) = \frac{\partial}{\partial y}\left(\frac{-4\sigma^*}{3k^*}\frac{\partial T^4}{\partial T}\frac{\partial T}{\partial y}\right). \tag{8}$$

Upon substitution, we obtained

$$\frac{\partial q_r}{\partial y} = -\frac{16\sigma^* T_\infty^3}{3k^*}\frac{\partial^2 T}{\partial y^2}. \tag{9}$$

By using Eq. (9) and Eq. (3) can be written as

$$u\frac{\partial T}{\partial x} + v\frac{\partial T}{\partial y} = \frac{\kappa}{\rho C_p}\frac{\partial^2 T}{\partial y^2} + \frac{1}{(\rho C_p)}\left(1+\frac{1}{\beta}\right)\left(\frac{\partial u}{\partial y}\right)^2 + \frac{16\,\sigma^* T_\infty^3}{3k^*\rho C_p}\frac{\partial^2 T}{\partial y^2} + \frac{Q(x)(T-T_\infty)}{\rho C_p} \tag{10}$$

Introduce the following similarity variables:

$$\psi = \sqrt{\frac{2\nu x u_e}{m+1}}\, f(\eta),\ \eta = \sqrt{\frac{(m+1)u_e}{2x\nu}}\, y,\ \theta = \frac{T - T_\infty}{T_w - T_\infty} \tag{11}$$

Where the stream function ψ(x, y) is defined by the following relations:

$u = (\frac{\partial \psi}{\partial y})$ and $v = -(\frac{\partial \psi}{\partial x})$

From Eq. (11) in above equation, we can write

$$u = u_e(x)\ f'(\eta),$$
$$v = \sqrt{\frac{\nu(m+1)u_e}{2x}}\left[f + \left(\frac{m-1}{m+1}\right)\eta\, f'(\eta) \right] \quad (12)$$

These automatically satisfied continuity equation (1) and we obtained the following locally similarity ordinary differential equations:

$$\left(1+\frac{1}{\beta}\right) f''' + ff'' + \lambda\left(1 - f'^2\right) + \left(M^2 + K\right)\left(1 - f'\right) \pm \lambda_T \theta \sin\frac{\Omega}{2} = 0 \quad (13)$$

$$\theta'' + \frac{\Pr}{(1+R)} f\,\theta' - 2\lambda \Pr f'\theta + \Pr\left(1+\frac{1}{\beta}\right) Ec\left(f''\right)^2 + \left(2-\lambda\right)\Pr \varepsilon\theta = 0 \quad (14)$$

Together with the boundary conditions

$$f'(\eta) = \gamma,\ \ \theta'(\eta) = -Bi\left(1-\theta(\eta)\right) \quad at\ \eta = 0 \quad (15)$$

$$f'(\eta) = 1,\ \ \theta(\eta) = 0 \quad at\ \eta = 0\ at\ \eta \to \infty \quad (16)$$

Where $M^2 = \frac{2\sigma B_0^2}{\rho U_\infty (m+1)}$, $K = \frac{2\nu\phi x}{k_1(m+1)u_e}$,

$\mathrm{Re}_x = \frac{x u_e}{\nu}$, $Gr_x = \frac{2g\beta_T T_\infty x^3}{\nu^2(m+1)}$, $\lambda_T = \pm\frac{Gr_x}{\mathrm{Re}_x^2}$,

($\lambda_T > 0$ corresponds to assisting flow and $\lambda_T < 0$ is for opposing flow), $\Pr = \frac{\mu c_p}{\alpha}$, $Ec = \frac{u_e^2(x)}{c_p(T_w - T_\infty)}$,

$\varepsilon = \frac{Q_0}{c_p U_\infty}$, $\gamma = \frac{U_w}{U_\infty}$, $Bi = \frac{h_f}{k_f}\sqrt{\frac{2x\nu}{(m+1)u_e}}$,

$R = \frac{4\sigma^* T_\infty^3}{k k^*}$.

The skin friction coefficient Cf_x and local Nusselt number Nu_x are defined as

$$Cf_x = \frac{\tau_w}{\rho u_e^2}, Nu_x = \frac{x q_w}{k(T_w - T_\infty)} \quad (17)$$

Where τ_w and q_w are the wall skin friction and wall heat flux, respectively, defined by

$$\tau_w = \mu_B\left(1+\frac{1}{\beta}\right)\left[\frac{\partial u}{\partial y}\right]_{y=0}, q_w = -\left[\frac{\partial T}{\partial y}\right]_{y=0} \quad (18)$$

For engineering interest, physical quantities are the local the skin friction coefficient and local Nusselt number Cf_x, Nu_x given as

$$\left(\mathrm{Re}_x\right)^{1/2} Cf_x \sqrt{\frac{2}{(m+1)}} = \left(1+\frac{1}{\beta}\right) f''(0),$$
$$\left(\mathrm{Re}_x\right)^{-1/2} Nu_x \sqrt{\frac{2}{(m+1)}} = -\left(1+\frac{4}{3}R\right)\theta'(0). \quad (19)$$

The system of Eqs. (13) and (14) along with the corresponding boundary conditions (15) and (16) are solved numerically by using MATLAB bvp4c solver. (Shampine et al., (2000)). Results are computed and presented in tables graphically.

3. RESULTS AND DISCUSSIONS

In this section, the numerical results for velocity $f'(\eta)$ and temperature $\theta(\eta)$ with corresponding boundary conditions as well as skin friction coefficient $\left(1+\frac{1}{\beta}\right)f''(\eta)$ and Nusselt number $-\theta'(\eta)$ have been computed and presented graphically in Figs. 2–11. These results demonstrate the effects of Casson fluid parameter β, Pressure gradient parameter λ, magnetic parameter *M*, porosity parameter *K*, thermal buoyancy parameter λ_T, Prandtl number *Pr*, Eckert number *Ec*, radiation parameter *R*, Biot number *Bi*, heat generation/absorption parameter ε and moving wedge parameter γ.

Fig. 2 depict the effect of magnetic field parameter on velocity for $\lambda_T > 0$; $\lambda_T = 0$; $\lambda_T < 0$ cases. It is evident that rising values of magnetic field parameter leads to increase the fluid flow in both cases of assisting and opposing flows. M is the ratio of electromagnetic force to viscous force, therefore increasing values of M means decreasing the viscous force that results in reduction in velocity boundary layer thickness. If there is a less suppression of Lorentz force it leads to deprecation in temperature and development in velocity field with progressive values of magnetic field parameter.

Fig. 3 shows the effect of β on velocity profile for various values of λ_T. It is worth mentioning here that $\beta \to \infty$ corresponds to Newtonian fluid, ($\lambda_T > 0$) represents assisting flow,

($\lambda_T < 0$) denotes opposing flow and ($\lambda_T = 0$) is for force convection flow. It is found that velocity is an increasing function of β in all cases of λ_T . The reason behind this is that increase of β leads to decrease in yield stress P_y, and consequently, reduces momentum boundary layer thickness. It is also observed that velocity is higher in case of Newtonian fluid for assisting flow $\lambda_T > 0$.

Fig. 4 illustrates the effect of λ on velocity profile for Newtonian and Non- Newtonian fluids. It is noteworthy that ($\lambda > 0$) corresponds to decreasing pressure, $\lambda = 0$ represents flat plate case and $\lambda < 0$ shows increasing pressure case. It is observed that the fluid velocity increases when $\lambda < 0$, and reduces when $\lambda > 0$. Also, velocity is higher for Newtonian fluid as compared to Non- Newtonian fluid. Also, thickness of momentum boundary layer increases as λ increases.

Fig. 5 reveals the effect of K on velocity profile for various values of λ. It needs to mention that K = 0 represents non-porous medium, whereas $K \neq 0$ is for porous medium. Porosity is defined as the measure of void (or empty) spaces in a porous medium and is a fraction of the volume of voids over the total volume It is noticed that velocity of fluid is higher for higher values of K. Convection flows are often influenced by porosity and in result raise the fluid velocity.

Fig. 6 elucidates the effect of on γ velocity profile in porous and non-porous medium. It is worth to mention that $\gamma < 0$ corresponds to the case when wedge is moving opposite to the fluid motion, $\gamma = 0$ represents static or stationary wedge case and $\gamma > 0$ is the case when wedge and the fluid move in the same direction. It is observed that velocity is increasing function of γ. It is also noticed that velocity of the fluid merely squeezes closer and closer to the wall when wedge and fluid move in one direction through porous medium.

The ratio of the heat transfer coefficient to thermal conductivity of the fluid particles is low. This can lead to decrease the temperature field with existing of biot number, which is observed in Fig.7.

The influence of Ec on temperature profile for different values of λ_T is shown in Fig.8. It is seen that the temperature rises for increasing values of Ec for both assisting flow ($\lambda_T > 0$) and opposing flow ($\lambda_T < 0$). The reason behind this is that in moving fluid heat energy is stored because of frictional heating, which results in higher temperature. In addition to this, stronger viscous dissipative heat causes an increase in fluid temperature. And also noted that the temperature is more when the wedge is moving opposite in fluid direction when compared with the wedge is moving same in fluid direction.

The effect of thermal radiation parameter on temperature field for various values of c is shown in Fig.9. Rising values of thermal radiation decreases the temperature near the plate and slightly raises away the plate. It is also observed that the thermal radiation is highly in effective on $\gamma < 0$ case when compared with $\gamma > 0$, $\gamma = 0$ cases.

Fig.10 displays the effect of Pr on dimensionless temperature profile for moving wedge parameter γ . Fluid temperature increases close to the wall and then merely reduces for increasing values of Pr. As expected, rate of thermal diffusion is lowered as Pr increases. That is, higher values of Pr lead to decrease in thermal boundary layer thickness. Consequently falls. It is also noted that the temperature is high for $\gamma < 0$ case compared with the other cases.

Fig. 11 reveals the effect of γ on temperature profile in porous and non-porous medium. It is found that temperature is decreasing function of γ for both porous and non-porous cases. Also noted that the temperature remains almost same for K = 0 and K = 2 for the wedge and the fluid move in the same direction.

In order to check the validity of present method, the results are compared with results of existing literature, and shown in Table1. Table 1 illustrate the comparison of local skin friction coefficient for different values of m with the results Ishak et al., (2007) and Imran Ullah et al., (2016) and are found in excellent agreement. It is also observed from this table that local skin friction coefficient increases with the increase of m. Table 2 describes the variation of wall shear stress and heat transfer rate obtained from the present method for increasing values of pertinent parameters. The wall shear stress decreases with increasing values of β, M, R, K, Pr, Ec, ε and Bi, whereas it decreases with decreasing λ_T . The heat transfer rate decreases with increasing β, M, Pr, Ec, and ε and opposite trend is observed for γ. The heat transfer rate remains constant for K and λ_T .

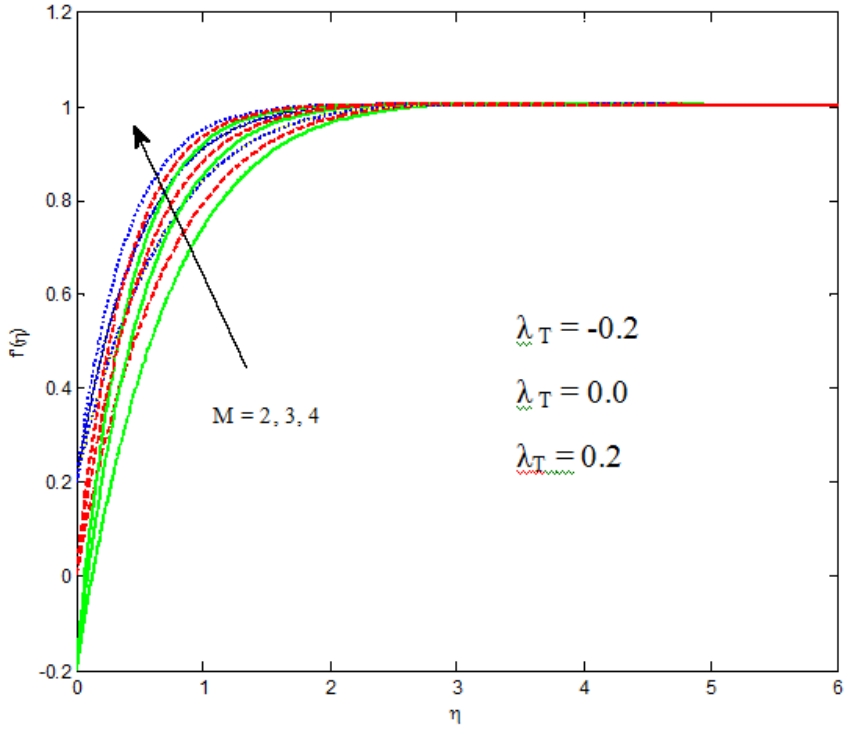

Fig.2 Effect of Magnetic field on velocity profiles for various λ_T

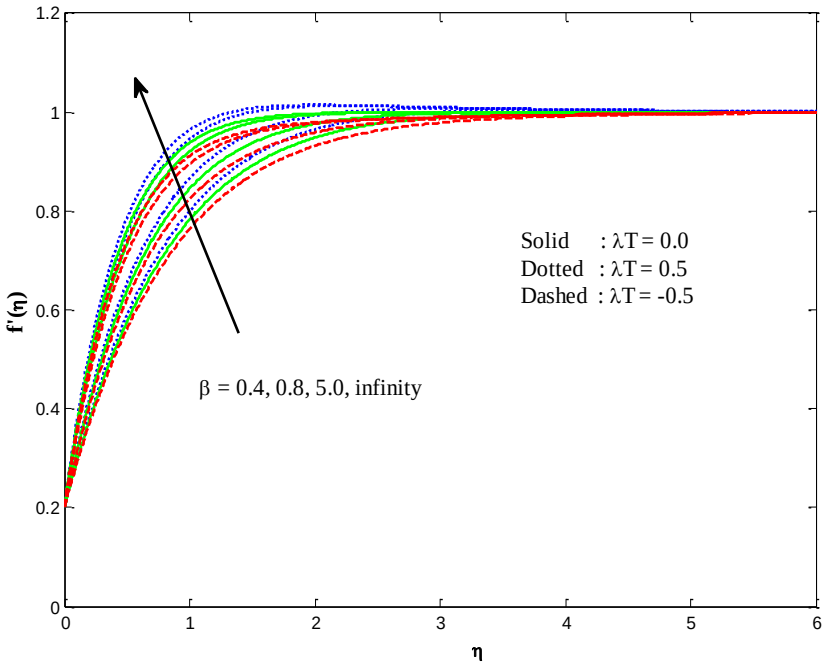

Fig.3 Effect of β on velocity for various λ_T

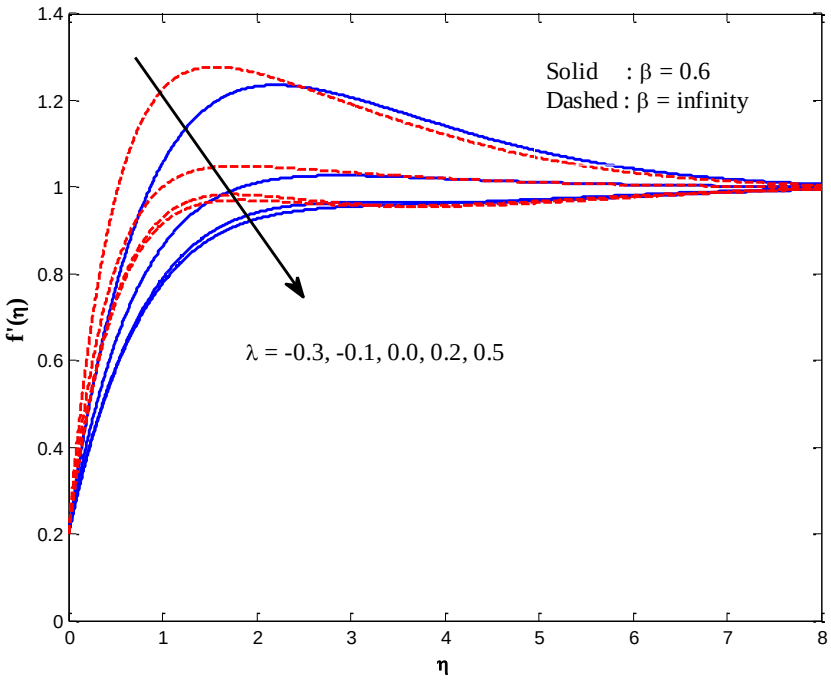

Fig.4 Effect of λ on velocity for different β

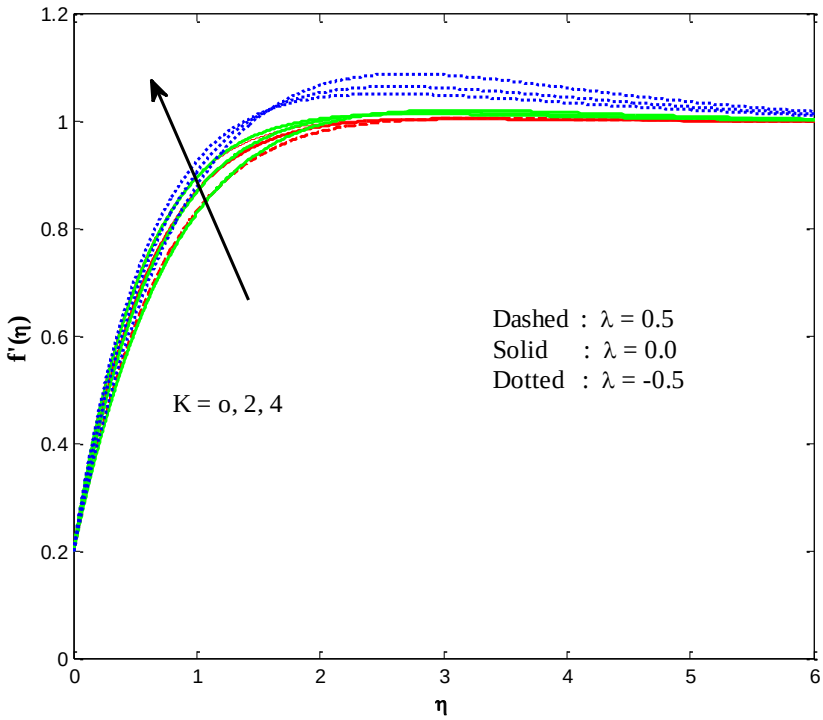

Fig.5 Effect of K on velocity for various λ

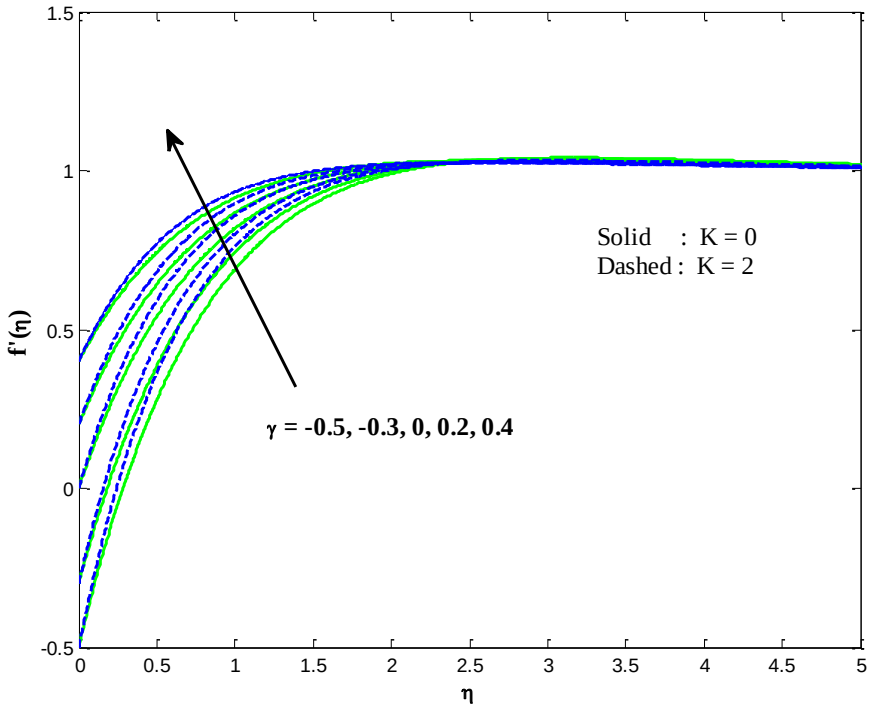

Fig.6 Effect of γ on velocity for various K

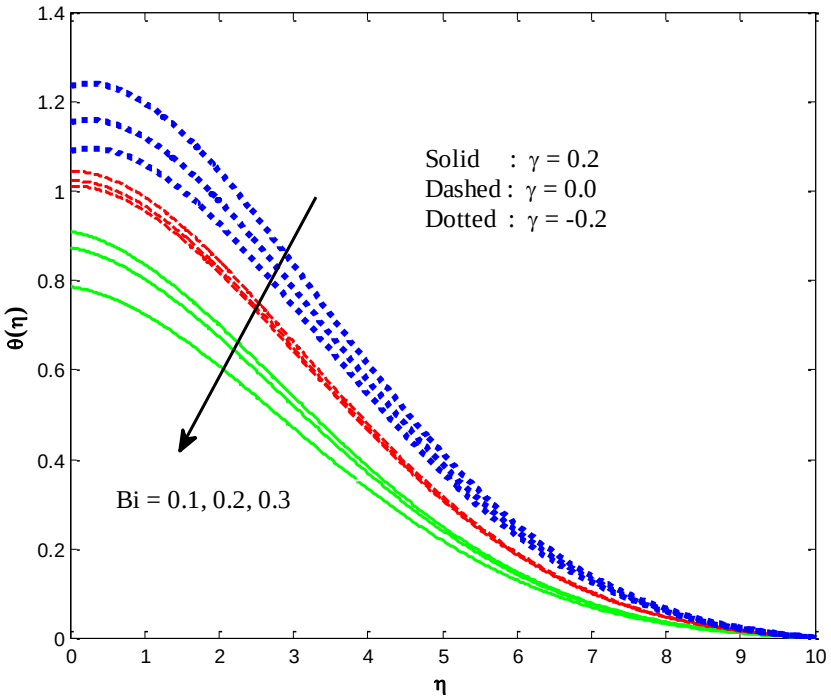

Fig.7 Effect of Bi on temperature field γ

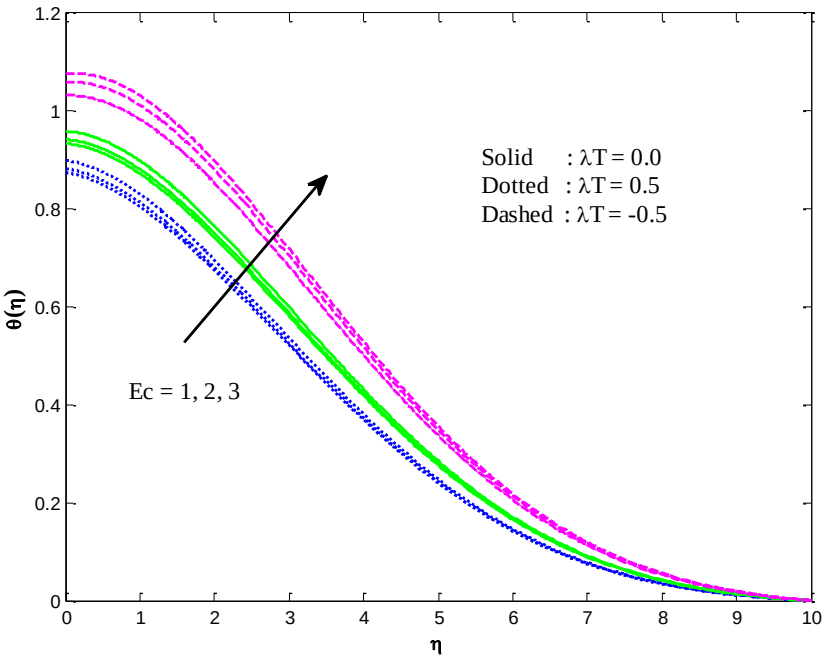

Fig.8 Effect of Ec on temperature for various λ_T

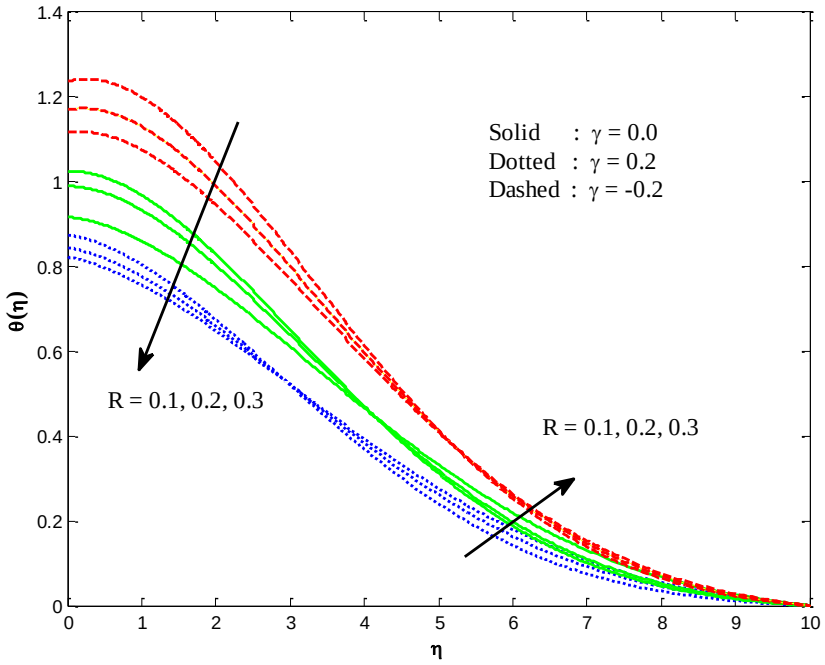

Fig.9 Effect of R on temperature field for various values of γ

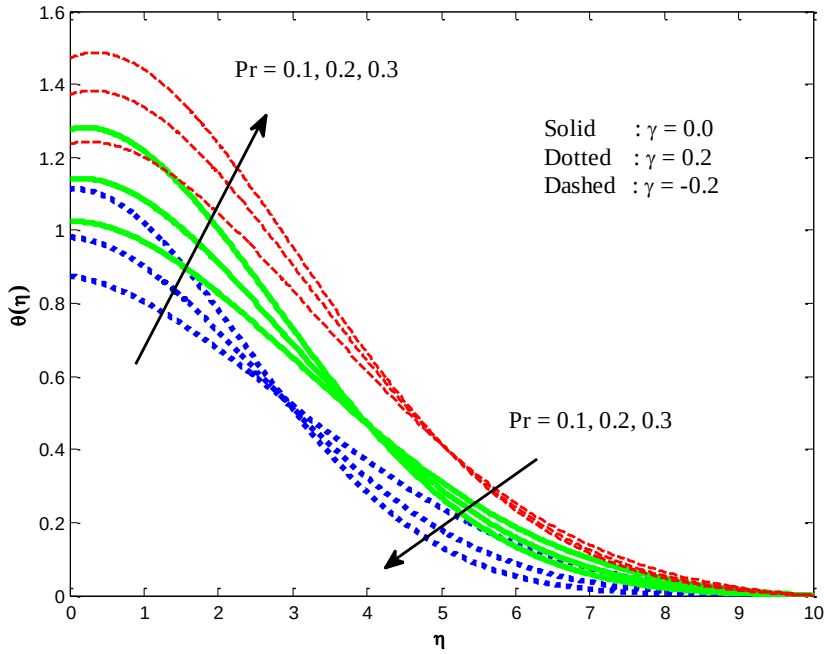

Fig.10 Effect of Pr on temperature field for various values of γ

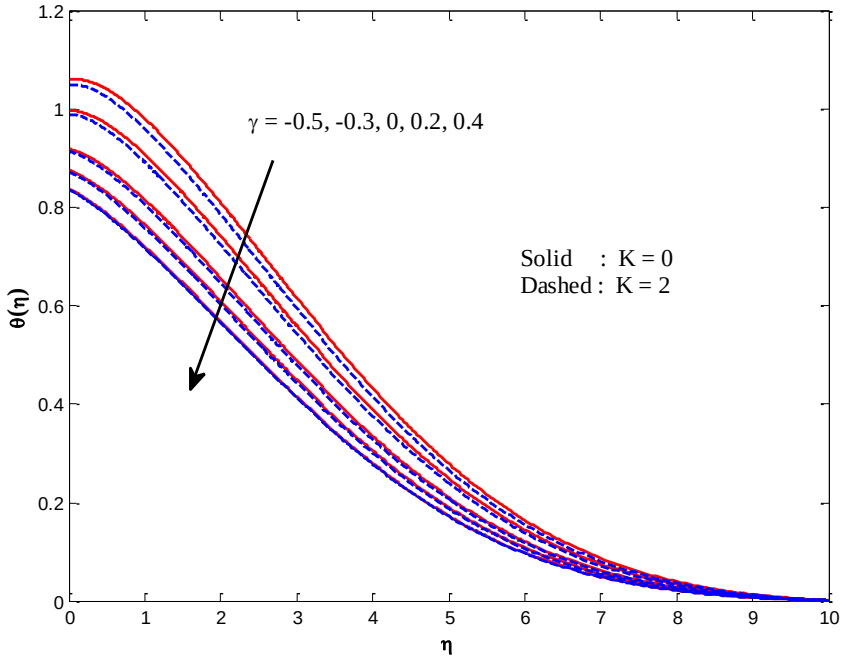

Fig.11 Effect of γ on temperature field for various values of K

Table 1. Comparison of coefficient of local skin friction $f''(0)$ for differet values of m with Pr = 0.73, M = K = λ_T = Ec = ε = γ = R = Bi = 0 and β→∞, where $\lambda = \frac{2m}{m+1}$

$f''(0)$			
m	Ishak et al.,(2007)	Imran Ullah et al.,(2016)	Present results
0	0.4696	0.4696	0.4691
1	1.2326	1.2326	1.2328
5	1.5504	1.5504	1.5504
100	1.6794	1.6794	1.6794
∞	1.6872	1.6872	1.6872

Table 2. Numerical results for skin friction coefficient and Nusselt number for different values of β, λ, M, K, λ_T, Pr, γ, Ec, ε, R and Bi.

β	λ	M	K	λ_T	Pr	γ	Ec	ε	R	Bi	$\left(1+\frac{1}{\beta}\right)f''(0)$	$-\theta'(0)$
0.6	0.5	2.0	0.2	0.5	0.1	0.2	1.0	1.0	0.1	0.2	3.0990	0.1117
0.9	0.5	2.0	0.2	0.5	0.1	0.2	1.0	1.0	0.1	0.2	2.7635	0.1097
1.2	0.5	2.0	0.2	0.5	0.1	0.2	1.0	1.0	0.1	0.2	2.3401	0.1045
0.6	1.0	2.0	0.2	0.5	0.1	0.2	1.0	1.0	0.1	0.2	3.2711	0.1270
0.6	1.5	2.0	0.2	0.5	0.1	0.2	1.0	1.0	0.1	0.2	3.4433	0.1366
0.6	0.5	4.0	0.2	0.5	0.1	0.2	1.0	1.0	0.1	0.2	5.4923	0.1097
0.6	0.5	6.0	0.2	0.5	0.1	0.2	1.0	1.0	0.1	0.2	8.0226	0.1061
0.6	0.5	2.0	0.4	0.5	0.1	0.2	1.0	1.0	0.1	0.2	3.1539	0.1117
0.6	0.5	2.0	0.6	0.5	0.1	0.2	1.0	1.0	0.1	0.2	3.2079	0.1117
0.6	0.5	2.0	0.2	0.0	0.1	0.2	1.0	1.0	0.1	0.2	2.9732	0.1118
0.6	0.5	2.0	0.2	-0.3	0.1	0.2	1.0	1.0	0.1	0.2	2.8976	0.1118
0.6	0.5	2.0	0.2	0.5	0.72	0.2	1.0	1.0	0.1	0.2	3.3473	-0.0584
0.6	0.5	2.0	0.2	0.5	1.0	0.2	1.0	1.0	0.1	0.2	3.5546	-0.2108
0.6	0.5	2.0	0.2	0.5	3.0	0.2	1.0	1.0	0.1	0.2	5.3736	-1.9349
0.6	0.5	2.0	0.2	0.5	0.1	0.0	1.0	1.0	0.1	0.2	3.8034	0.1060
0.6	0.5	2.0	0.2	0.5	0.1	-0.2	1.0	1.0	0.1	0.2	4.4893	0.0991
0.6	0.5	2.0	0.2	0.5	0.1	0.2	2.0	1.0	0.1	0.2	3.1087	0.1055
0.6	0.5	2.0	0.2	0.5	0.1	0.2	5.0	1.0	0.1	0.2	3.1383	0.0866
0.6	0.5	2.0	0.2	0.5	0.1	0.2	1.0	1.5	0.1	0.2	3.1260	0.0959
0.6	0.5	2.0	0.2	0.5	0.1	0.2	1.0	2.0	0.1	0.2	3.1692	0.0708
0.6	0.5	2.0	0.2	0.5	0.1	0.2	1.0	1.0	0.3	0.2	3.0956	0.1139
0.6	0.5	2.0	0.2	0.5	0.1	0.2	1.0	1.0	0.6	0.2	3.0922	0.1161
0.6	0.5	2.0	0.2	0.5	0.1	0.2	1.0	1.0	0.1	0.3	3.1258	0.1391
0.6	0.5	2.0	0.2	0.5	0.1	0.2	1.0	1.0	0.1	0.5	3.1590	0.1729

4. CONCLUSIONS

Thermal radiation with combination of viscous dissipation and heat generation has many real time engineering as well as industrial applications. Owing view into this Falkner-Skan flow of radiative Magnetohydrodynamic Casson fluid past a static/moving wedge through porous medium in the presence of convective boundary condition is studied. The arising sets of nonlinear differential equations have been numerically solved by MATLAB bvp4c solver. For engineering purpose, we also computed the

friction factor coefficient and local Nusselt number. The conclusions are as follows:

- Fluid flow increases with the increase of M, K, γ and β.
- Fluid velocity decreases with increase of λ.
- Fluid temperature increases with increase of Ec and Pr.
- Fluid temperature decreases with increase of Bi, R and γ.
- The wall shear stress decreases with increasing values of β, R, K, Pr, Ec, ε and Bi, whereas it decreases with decreasing λ_T .
- The heat transfer rate decreases with increasing β, Pr, Ec, and ε and opposite trend is observed for γ.

Acknowledgements
The first author gratefully acknowledged by UGC scheme MANF. Award letter F1-17.1/2017-18/MANF-2017-18-AND-77291 / (SA-III/Website).

REFERENCES

[1] Abdulhameed, M., Saleh, H., Hashim,I., and Roslan, R. (2015): Radiation effects on two-dimensional MHD falkner-skan wedge flow, Appl Mech Mater.,vol.773–774, pp.368–372. doi:10.4028/www.scientific.net/AMM.773-774.368

[2] Anuar Ishak, Roslinda Nazar, and Ioan Pop. (2009): MHD boundary - layer flow of a micropolar fluid past a wedge with constant wall heat flux, Commun.Nonlinear Sci. Numer. Simul, vol.14, pp.109–118. https://doi.org/10.1016/j.cnsns.2007.07.011

[3] Anuar Ishak, Roslinda Nazar, and Ioan Pop, (2007): Falkner-Skan equation for flow past a moving wedge with suction or injection, J. Appl. Math.Comput., vol. 25, No. 1, pp.67–83.

[4] Imran Ullah, Ilyas Khan, and Sharidan Shafie, (2016): Hydromagnetic Falkner-Skan flow of casson fluid past a moving wedge with heat transfer, Alexandria Engineering Journal., vol.55, pp.2139–2148. https://doi.org/10.1016/j.aej.2016.06.023

[5] Leal, L.G., (2007): Advanced transport phenomena: fluid mechanics and convective transport processes, Cambridge University Press, New York.

[6] Makungu James, Mureithi, E.W., and Dmitry Kuznetsov. (2015): Effects of variable viscosity of nanofluid flow over a permeable wedge embedded in saturated porous medium with chemical reaction and thermal radiation, International Journal of Advances in Applied Mathematics and Mechanics,vol.2, No.3, pp.101 – 118.

[7] Mourad F.Dimian, (2004): Effect of the magnetic field on forced convection flow along a wedge with variable viscosity, Mechanics and Mechanical Engineering., vol.7, No. 1, pp.107–120.

[8] Nabil T. El-Dabe, Ahmed Y.Ghaly, Raafat R.Rizkallah, Karem M. Ewis, and Ameen S. Al-Bareda, (2015): Numerical solution of MHD boundary layer flow of non-newtonian casson fluid on a moving wedge with heat and mass transfer and induced magnetic field ,J. Appl. Math. Phys., vol. 3, pp.649-663.

[9] Prasad, K. V., Datti, P. S., and Vajravelu, K. (2013): MHD Mixed convection flow over a permeable non-isothermal wedge, Journal of King Saud University Science., vol. 25, pp. 313–324. https://doi.org/10.1016/j.jksus.2013.02.005

[10] Raju, C.S.K., and Sandeep, N. (2016): Nonlinear radiative magneto hydrodynamic Falkner-Skan flow of casson fluid over a wedge, Alexandria Engineering Journal, vol.55, No. 3, pp.2045-2054.

[11] Rashid Ahmad, and Waqar Ahmed Khan, Effect of viscous dissipation and internal heat generation/absorption on heat transfer flow over a moving wedge with convective boundary condition, (2013): Heat Transfer—Asian Research.,vol.42, No.7,pp. 589–602. Doi :10.1002/htj.21055

[12] Schlichting, H., and Gersten, K. (2000): Boundary Layer Theory, Eighth revised Ed., Springer-Verlag, Berlin.

[13] Shampine, L.F., Kierzenka, J., and Mark W Reichelt, (2000): Solving Boundary Value Problems for Ordibary Differential Equations in MATLAB with Bvp4c, pp.1-27.

[14] Suneetha, S., Bhaskar Reddy, N. and Ramachandra Prasad, V. (2008) Thermal radiation effects on MHD free convective flow with variable surface temperature and concentration, Journal of Naval Architecture and Marine Engineering., Vol.2,pp.57-70. DOI: 10.3329/jname.v5i2.2694

[15] Suneetha, S., Bhaskar Reddy, N., (2010): Radiation and mass transfer effects on MHD free Convection flow past a moving vertical cylinder embedded in porous medium, Journal Of Naval Architecture and marine Engineering., Vol. 7, No.1,pp.1-10. http://dx.doi.org/10.3329/jname.v7i1.2901